PREPARATION AND CRYSTALLINE MICROSTRUCTURE OF RAPIDLY SOLIDIFIED NEW AMORPHOUS Al-Fe-V-Si-Mm ALLOY①

Wang Jianqiang, Gu Tao, Zeng Meiguang, Chen Xiufang, Zhang Baojing
Department of Materials Science, Institute of Science, Northeastern University, Shenyang 110006

ABSTRACT A new metallic glass of Al-riched Al-Fe-V-Si-Mm alloy was firstly produced by liquid quenching. The microstructural features of as-cast and crystallization were studied by DSC, XRD, TEM and EDX. During the process of annealing crystallization this amorphous alloy went through three stages with the precipitation of α- Al particles, $Al_{11}(La, Ce)_3$ particles and i- phase, finally the i'- phase. It was also observed that the size of four kinds of phases was less than 100 nm at 718 K for 1 h. The dominant factors for the formation of amorphous Al-Fe-V-Si-Mm and good thermal stability are the strong attractive interaction between Al and Mm and size differentia effect.

Key words rapid solidification Al-Fe-V-Si-Mm alloy amorphous phase annealed crystallization microstructure

1 INTRODUCTION

Amorphous metals have attracted considerable attention in recent years in view of their importance for technological applications. These materials exhibit interesting magnetic properties combined with high mechanical strength, extreme hardness and resistance to corrosion. It has recently been found that Al-based alloys with high tensile fracture strengths exceeding 1 000 MPa were obtained by rapid solidification in nonequilibrium structure states of an amorphous single phase[1, 2], amorphous plus nanoscale *fcc*- Al phases[3, 4] and nanoscale *i*- cosahedral plus Al phases[5, 6]. The specific strength defined by the ratio of tensile fracture strength to density is expected to show the highest value for the mixed icosahedral and Al phase. Thus, it is very important for the icosahedral and Al phase to search a new alloy system in a lower solute concentration range. In this study attention was focussed on the new amorphous Al-Fe-V-Si-Mm preparation by adding misch metal to dispersion-strengthed Al-Fe-V-Si alloy and microstructural changes during annealing treatment.

2 EXPERIMENTAL PROCEDURE

An $Al_{87.3}Fe_{4.3}V_{0.7}Si_{1.7}Mm_{6.0}$ (%) alloy was melted by a mixture of Al-48.4% V master alloy and other purified metals. The misch (Mm) metal contained 55% Ce, 29% La, 11% Nd and 5% Pr. Melt spining was carried out under an argon atmosphere using a copper wheel (20 cm in diameter) with a typical circumferential velocity 25 m/s. The ribbon dimensions were 30 to 40 thick and 2 mm wide. The crystallization studies of the melt-spun alloy were carried out in a differential scanning calorimeter (DSC) with different heating rates of 5, 10, 20 and 40 K min^{-1}. The as-cast and annealed phase constitution were characterized by X-ray diffractometer (XRD) and energy dispersive X-ray (EDX) and transmission

① Supported by the National Natural Science Foundation of China; Received Nov. 22, 1994

electron microscopy (TEM) techniques.

The TEM samples were prepared by thinning electrolytically the ribbons in a solution of 25% nitric acid and 75% methanol at a temperature of −40 ℃. The TEM used in this work was a JEOL-100 CX operating at 100 kV. An electron microscopy specimen heating holder (EM-SHH) was used to heat the foils in the TEM during observation. The temperature was measured by a Pt/Pt~10% Ph thermocouple.

3 RESULTS AND DISCUSSION

3.1 *Continuous Heating Experiments*

To characterize the thermal stability of as-cast glass, the DSC curves at different heating rates are shown in Fig. 1. When this amorphous alloy was continuously heated, three exothermic peaks corresponding to different crystallization temperatures were apparent. At a heating rate of 10 ℃/min these temperatures were 503(T_{p1}), 623(T_{p2}) and 718 K(T_{p3}), respectively. This fact indicates that more than one crystallization process occurs until all the material becomes crystalline.

Measuring the peak positions at different heating rates, it can be used to determine the activation energies for the different reaction steps by the Kissinger method[7] i.e. from the slope of the curves of $\ln(T_p/\dot{T})$ against $1/RT_p$, where T_p is the peak temperature and $\dot{T}$ the heating rate. Fig. 2 shows the corresponding plots for the three peaks of the DSC curves. The activation energies for the first peak (E_{ac1} = 332 kJ/mol) is higher than that for the second peak (E_{ac2} = 261 kJ/mol) and the third peak (E_{ac3} = 222 kJ/mol).

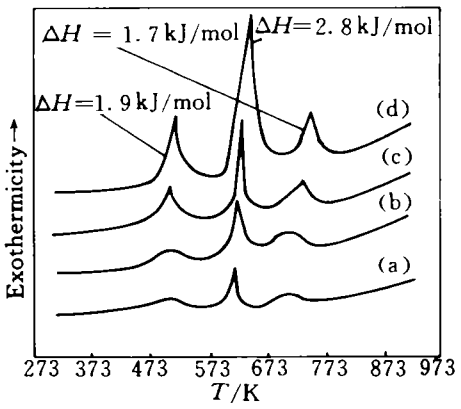

Fig. 1 DSC curves of amorphous $Al_{87.3}Fe_{4.3}V_{0.7}Si_{1.7}Mm_{6.0}$ alloy
(a)—5 K/min; (b)—10 K/min; (c)—20 K/min; (d)—40 K/min

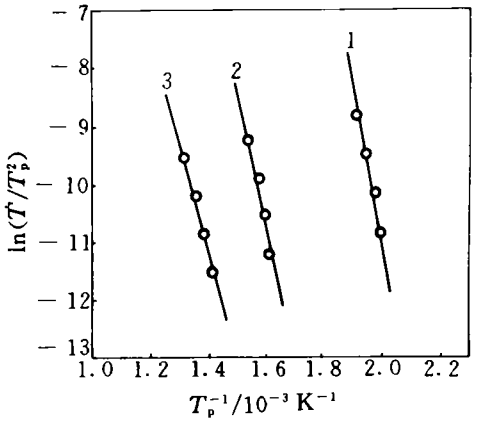

Fig. 2 The Kissinger plots of calculating the activation energy of three exothermic peaks for amorphous
1—first peak; 2—second peak; 3—third peak

3.2 *Phase Transformation During Crystallization*

The structure of phases present in the investigated alloy after isothermal annealing at different temperatures, was determined by XRD and TEM. Table 1 lists the XRD data of the annealing crystallization products. The isothermal crystallization process can be concluded as follows:

$$AM \xrightarrow{513K} AM' + \alpha\text{-}Al \xrightarrow{618K} \alpha\text{-}Al + Al_{11}(La, Ce)_3 + i\text{-phase} \xrightarrow{718K} \alpha\text{-}Al + Al_{11}(La, Ce)_3 + i\text{-phase} + i'\text{-phase}$$

where intermetallic $Al_{11}(La, Ce)_3$ compound belongs to orthorhombic structure, the diffraction position of quasicrystalline i and i'-phase is very similar to the results on Al-Ce-M (M≡V, Cr, Mo, Mm, Fe)-Si alloys reported by Inoue and his co-workers[8].

Table 1 X-ray diffraction data for crystallization products of Al-Fe-V-Si-Mm glass

513K, 1h			618K, 1h		718K, 1h	
d/nm	I/I_{max}		d/nm	I/I_{max}	d/nm	I/I_{max}
					0.507+	11
			0.406+	19	0.406+	18
			0.402+	18	0.402+	19
					0.319**	39
			0.312+	14	0.312+	12
			0.280*	31	0.280*	54
			0.269+	22	0.269+	22
			0.268+	21	0.268+	22
			0.265+	43	0.265+	39
			0.244*	31	0.244*	22
0.235	100	Al	0.235	100	0.235	100
					0.225**	62
					0.221**	18
					0.212**	22
0.202	50	Al	0.202	51	0.202	54
					0.184+	9
			0.171+	11	0.171+	8
			0.170+	11	0.170+	8
					0.160**	23
0.142	29	Al	0.142	19	0.142	30
					0.135**	16

+—$Al_{11}(La, Ce)_3$; * — i- phase; * * — i'- phase

Fig. 3(a) — (e) show TEM micrographs and diffraction patterns for the material in the as-quenched and annealed states. It confirms the results of XRD about the coexistence of α-Al, $Al_{11}(La, Ce)_3$, i- phase and i'- phase annealing for 1 h at 718 K. Moreover, it is noticeable that the sizes in any kind of phase are less than 100 nm in the temperature range of 513 K to 718 K. Judging from the EDX spectra for region ① to ④ corresponding to Fig. 3(c), it is clear that the stoichiometric i- phase is about $Al_2(Fe, V)Si_{12}$. However, i'- phase is a compound of two kinds of particles, their chemistries are $Al_{24}(Fe_1, V)Si_{18}$ and $Al_{40}(Fe, V)Si_2$, respectively. In addition, about the Fe concentration contrasting region ① to region ④, it appears that the Fe content in large particles (about 0.581%) is much lower than that in surrounding area (about 5.966%). So we can infer that the significant effects were produced to usual Al-Fe-V-Si alloy with the Mm additions.

3.3 *In Situ* TEM *Observation*

In order to investigate the micromechanism for crystallization of Al-Fe-V-Si-Mm amorphous alloy, *in situ* observation method was used to yield the phase transformation information while several phases were coexistent. After a glassy Al-Fe-V-Si-Mm foil was placed on a specimen heating holder in the TEM, it was heated to 718 K, holding the temperature, when the annealing time reached about 5 min, many small clusters (or particles) appeared in the amorphous matrix (Fig. 4(a)). The average size of these clusters was up to 10～50 nm. Selected area electron diffraction (SAED) corresponding to this zone showed that the randomly distributed clusters consist of several kinds of phases, as indexed in Fig. 3(d)～(f).

With the annealing time increasing from 5 min to 20 min, a close dynamic observation of the phase gathering was shown in Fig. 5(a)～(d). It can be found that the phase gatherings have taken place not only in the same kinds of phases but also in the different kinds of phases (indicated by arrow *A*, *B*, *C*). Several groups of small crystalline particles were ahead of the large crystalline particles front. The large particle front moved and touched the small particles, and then passed them.

The experimental phenomena discribed above could be explained as follows. During these phases growth process, the small particles were changed in their orientations (called "shearing") and deposited onto the growing large particles front[9]. On the other hand, the orientation and configuration of the final gathering phases are different from that of the original large crystalline particles.

3.4 *Role of Misch Metal*

The equilibrium phase diagrams[10] of Al-Ce(La, Fe, Ni, Nb, Ba, Ca) binary alloys indicate that the solute concentrations and melting tempertures of intermetallic compounds $Al_{11}Ce_3$ and $Al_{11}La_3$ in Al-rich composition ranges corresponding to the magnitude of at-

tractive interaction (mixing energy) are, respectively, 21.4% and 1493K for La and 21.4% and 1508K for Ce. The minimum solute concentration (21.4%) for formation of the Al-Ce (La) compounds is lower than that (25%) of Al-M(M≡Fe, Ni, Nb, Ba, Ca) binary alloy, and the melting temperatures of $Al_{11}Ce_3$ and $Al_{11}La_3$ are much higher than those (973 to 1373K) of Al_4Ba, Al_4Ca and Al_9Co_2 with solute concentrations below 25%. These data allow us to conclude that the magnitude of attractive interaction between Al and solute metal is considerably larger for Ce and La than for the other solute metals. While

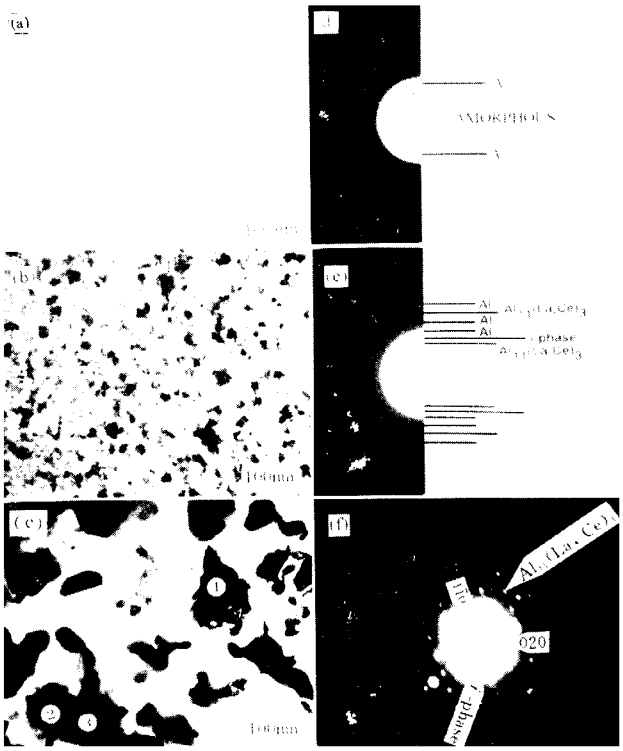

Fig. 3 TEM micrographs and SADPs of annealed Al-Fe-V-Si-Mm amorphous alloy
(a), (d)—as-quenched; (b), (e)—618K, 1h; (c), (f)—718K, 1h
Zone ① $Al_{32}(Fe, V)Si_{12}+Al_{11}(La, Ce)_3$; Zone ②—$Al_{24}(Fe, V)Si_{18}+Al_{11}(La, Ce)_3$;
Zone ③—$Al_{40}(Fe,V)Si_2+Al_{11}(La, Ce)_3$; Zone ④—surrounding area

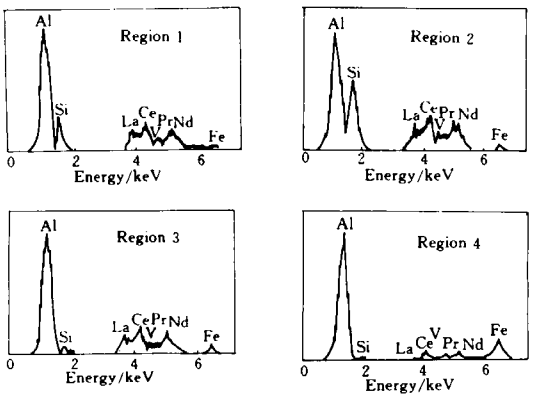

Fig. 4 EDX spectra taken from region 1～4 in the Fig. 3

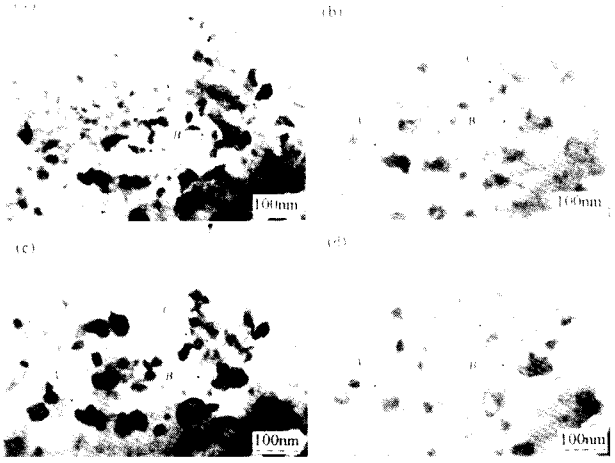

Fig. 5 Phase gatherings of the glassy Al-Fe-V-Si-Mm foil *in situ* annealed at 718 K
(a)—5 min; (b)—10 min; (c)—15 min; (d)—20 min;
A—*i'* -phase (L) and $Al_{11}(La, Ce)_3$(S); *B*—*i* -phase (L) and $Al_{11}(La, Ce)_3$(S)
C —two $Al_{11}(La, Ce)_3$ particles. L—large, S—small

adding the Mm to original Al-Fe-V-Si alloy the attractive bonding natures between Al and Ce (La) become the most dominant factor among several interactions. The strongest interaction increases the shear viscosity of the molten alloy and the energy for preventing atom coordinating redistribution, resulting in a high resistance to nucleation and crystallization.

Besides the attractive interaction there is size differentia effect between Al and Mm. Generally larger size differentia of constituent atoms ($>10\%$) can further enhance close atom stack and suppress the crystal growth, thus improving glass formation and thermal stability. The difference in atom size between Al(1.43 Å) and La(1.877 Å), Ce(1.824 Å), Pr(1.828 Å) Nd(1.821 Å) is up to 27%. So it may be concluded that the glass formation in Al-Fe-V-Si-Mm alloy results from the simultaneous satisfaction of the two factors of a strong attractive interaction and large size differentia effect between Al and Mm.

4 CONCLUSION

(1) $Al_{87.3}F_{4.3}V_{0.7}S_{1.7}Mm_{8.0}$ amorphous alloy was first prepared by using melt-spinning technology.

(2) The results of this study indicate that Al-Fe-V-Si-Mm glass crystallizes in three steps:

$$AM \xrightarrow{513K} AM' + \alpha\text{-}Al \xrightarrow{618K} \alpha\text{-}Al + Al_{11}(La, Ce)_3 + i\text{-phase} \xrightarrow{718K} \alpha\text{-}Al + Al_{11}(La, Ce)_3 + i\text{-phase} + i'\text{ phase}.$$

(3) Nanoscale α-Al, $Al_{11}(La, Ce)_3$ and i-phase were obtained for glass ribbons aged at 618K for 1h. No α-$Al_{13}(Fe,V)_3Si$ particles were observed in the whole process of crystallization.

REFERENCES

1 Inoue A *et al.* Jpn J Appl Phys, 1988, 27: 1479.
2 Tsai A P *et al.* Metall Trans, 1988, 19A: 1369.
3 Inoue A *et al.* Mater Trans, JIM, 1993, 34: 87.
4 Kim Y H *et al.* J Japan Inst Light Metal, 1992, 42: 217.
5 Inoue A *et al.* Mater Trans, JIM, 1992, 33: 669.
6 Inoue A *et al.* Mater Trans, JIM, 1992, 33: 723.
7 Kissinger H E. Anal Chem, 1957, 29: 1702.
8 Watanabe M *et al.* Mater Sci Eng, 1994, A179/A180: 661.
9 Lu K *et al.* Acta Metall Sinica, 1991, 27: B33.
10 Massalski T B. Binary Alloy Phase Diagram, Metals Park, Ohio: ASM, 1986, 1: 125.

(Edited by Zhu Zhongguo)